



Enhanced Performance of Micro-Electro-Mechanical-Systems (MEMS) Microbial Fuel Cells Using Electrospun Microfibrous Anode and Optimizing Operation

A. Fraiwan¹, S. Sundermier¹, D. Han², A. J. Steckl², D. J. Hassett³, S. Choi^{1*}

¹ Bioelectronics and Microsystems Laboratory, Department of Electrical and Computer Engineering, SUNY Binghamton, 4400 Vestal Pkwy, Binghamton, NY 13902, USA

² Nanoelectronics Laboratory, School of Electronic and Computing Systems, University of Cincinnati, 839 Rhodes Hall, Cincinnati, OH 45221, USA

³ Department of Molecular Genetics, Biochemistry and Microbiology, University of Cincinnati College of Medicine, 231 Albert Sabin Way, Cincinnati, OH 45267, USA

Received December 07, 2012; accepted April 09, 2013; published online April 30, 2013

Abstract

In this work, a microfabricated anode based on gold coated poly(ϵ -caprolactone) fiber was developed that outperformed gold microelectrode by a factor of 2.65-fold and even carbon paper by 1.39-fold. This is a result of its ability to three-dimensionally interface with bacterial biofilm, the metabolic “engines” of the microbial fuel cell (MFC). We also examined unavoidable issues as the MFC is significantly reduced in size (e.g. to the microscale); (1) bubble production or movement into the microchamber and (2) high sensitivity to flow rate variations. In fact, intentionally induced bubble

generation in the anodic chamber reduced the MFC current density by 33% and the MFC required 4 days to recover its initial performance. Under different flow rates in the anode chamber, the current densities were almost constant, however, the current increased up to 38% with increasing flow rate in the cathode.

Keywords: Air Bubbles, Electrospinning, Flow Rate, MEMS Microbial Fuel Cell (MFC), Microchamber, Poly(ϵ -Caprolactone) (PCL) Fiber, *Shewanella Oneidensis* MR-1

1 Introduction

Driven by increasing concerns over the energy-climate crisis and environmental pollution, microbial fuel cells (MFCs) are a major focus as a potential source for renewable energy production. A MFC can transform the chemical energy of biodegradable organic matter into electrical power catalyzed by bacterial metabolism on an anode. Typically, an MFC is comprised of an anode chamber and cathode chamber separated by a proton exchange membrane (PEM), which permits H^+ , or other cations, to pass through from the anode chamber to the cathode chamber [1]. With the successful validation of conceptual macro-sized MFCs as a low-cost renewable and self-sustainable energy technology, recent research has focused on miniaturizing MFCs for use in powering small portable electronics [2–7]. However, existing micro-sized MFCs are generally limited by their relatively low power density rendering them insufficient for practical applications

[4, 7]. Their power density is about six orders of magnitude lower than that of macro-sized MFCs ($690 \mu W cm^{-2}$), ranging from power densities of only 0.0023 to $0.4 \mu W cm^{-2}$ [7, 8]. Recently, Choi et al. [9, 10] reported that an oxygen impermeable interface and anode chamber depth were the significant limiting factors in designing MEMS MFCs. This is because (1) bacteria tend to consume oxygen without transferring electrons to the anode and (2) the space constraint with shallow anode chamber depth can limit the thickness of the biofilm, thereby decreasing current generation. They achieved a high power density micro-sized MFC by optimizing the anode chamber depth and minimizing oxygen invasion into the anode chamber. The maximum power density of their MFC was $95 \mu W cm^{-2}$, the highest value among previously reported micro-sized MFCs, and even comparable to that of

[*] Corresponding author, sechoi@binghamton.edu

their macro-scale counterparts [10]. Despite these impressive figures, the performance of micro-sized MFCs still remains insufficient for full realization of their potential applications.

One major factor that limits performance involves the anode material. It has been reported that the significant loss of energy at the anodic surface/compartments is the main energy bottleneck in the MEMS MFC, causing high internal resistance [9]. Many MEMS MFCs used gold as an electrode material, since gold is biocompatible, highly conductive, and is compatible with conventional microfabrication methods [5]. However, their results with *Geobacter sp.* and other studies with *Shewanella sp.* suggested that bare gold is a poor electrode material for the anode of MFCs because gold lacks functional groups, such as quinones, a natural electron acceptor for anaerobic respiration [11, 12]. The best electrodes used in macro-sized MFCs have been carbon-based materials, such as graphite, carbon paper/cloth, etc., due to their large surface area and functional organic groups favoring cell viability as well as ease of handling [5, 11, 13, 14]. As a result, the best output and stability have been reported from MFCs with carbon-based anodes [15]. However, the intrinsic advantages of traditional carbon anodes have not yet been translated to micro-sized MFCs, as these materials are bulky and not compatible with microfabrication [5]. Moreover, carbon papers with two-dimensional structure have limited bacterial loading capacity and robust biofilm formation. If one can identify alternative electrode materials meeting MEMS process requirements and providing better surface characteristics for bacterial biofilm formation, the power density of MEMS MFC will increase substantially and also potentially standardize a platform for microfabrication of micro-sized MFCs [4]. One proposed strategy for MEMS MFC anode is to use carbon nanotubes, which increase the surface area and the conductivity of the anode [16]. Here, we proposed a macroporous MEMS anode-based on gold coated poly(ϵ -caprolactone) (PCL) fiber. Its performance was compared with micro-sized MFCs using different conventional anode materials; gold and carbon paper.

Other major factors that limit MEMS MFC performance involve unavoidable issues as the effective chamber volumes of the MFCs are reduced to the microliter regime; (1) air bubble interruption and (2) high sensitivity to flow rate variation. Currently, these limiting factors need to be studied because the lack of knowledge and information on these subjects presents critical issues when developing and operating MEMS MFCs. First, the potential invasion of air bubbles into the microchambers will be directly related to the power generation as the trapped bubbles normally occupy significant chamber volume and likely hamper bacterial growth and their subsequent electron transfer. In addition, it is difficult to remove trapped bubbles in the microfluidic chambers leading to continuous interruption. In this work, we intentionally introduce air bubbles into each chamber and measure the power density. Second, the effect of flow rate on performance might be significant relative to macro-sized MFCs since the minute variations in flow rate largely affect changes in mass

transfer flux and reaction kinetics. Here, we observed the current densities for the different flow rates of anolyte and catholyte.

2 Materials and Methods

2.1 Operating Principle

The basic structure of a MFC consists of two chambers; the cathode and the anode separated by a PEM. The two electrodes are connected *via* a conductive load to complete the external circuit. In the anode, bacteria oxidize organic matter and then complete respiration by transferring the electrons to the anode *via* extracellular electron transfer (EET). During the process, chemical energy is captured throughout the electron transport chain. Nicotinamide adenine dinucleotide (NAD⁺) and nicotinamide adenine dinucleotide dehydrogenase (NADH) function as the coenzymes for the reactions are repeatedly oxidized and reduced to prompt the synthesis of the biological energy unit, adenosine triphosphate (ATP). Electrons that are transferred to the anode flow to the cathode through the external resistor. The redox couple is complete when captured electrons reduce ferricyanide, $[\text{Fe}(\text{CN})_6]^{3-}$ at the cathode [4].

2.2 Inoculum

Wild-type *Shewanella oneidensis* was grown in L-broth medium as the anolyte, while a phosphate-buffered ferricyanide (50 mM, pH 7.0) was used as the catholyte. To date, two major families of bacteria, *Geobacter sp.* and *Shewanella sp.* have been used in MEMS MFCs because of their well-known EET mechanisms and metabolic diversity [4, 9]. Although unique aspects of *Geobacter sp.* have led to much higher power densities in MEMS MFCs [10], metabolic diversity and flexibility continues to drive significant research on *Shewanella sp.* [17]. The primary focus area in this family is the wild type strains *Shewanella oneidensis* MR-1 [18]. L-broth media contained 10.0 g triptone, 5.0 g yeast extract and 5.0 g NaCl per liter. Anolyte and catholyte solutions were continuously supplied using a syringe pump at a rate 1.0 $\mu\text{L min}^{-1}$ unless otherwise specified and the MFC was operated at 30 °C.

2.3 Device Assembly

Our MFC contains vertically stacked 50 μL anode and cathode chambers separated by a PEM (Nafion 117). Each layer except for the PEM was micro-patterned by using laser micromachining and was precisely aligned. Each chamber volume was defined by a 500 μm -thick patterned gasket. The exposed anode/cathode area was 100 mm^2 . Figure 1a shows the schematic diagram of the MFC used in these studies. Photo-images of the fully assembled MFC and the individual layers are shown in Figure 1b and c, respectively. Three MEMS MFCs were prepared with different anode materials; gold (sputtered), gold-coated PCL fiber and carbon paper

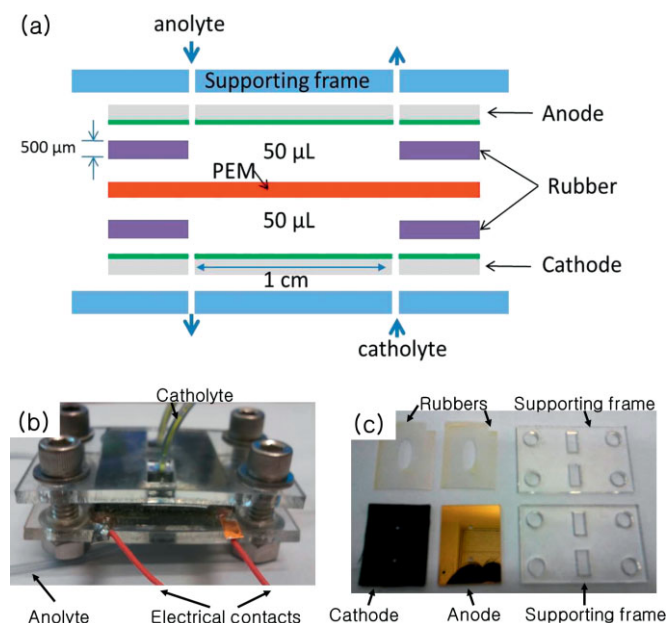


Fig. 1 (a) Schematic of our MEMS MFC, (b) fully assembled MEMS MFC, and (c) individual layers of the MFC.

(Fuel Cell Store, 0.48 g cc^{-1} , 0.2 mm). Each anode was prepared on $4 \text{ cm} \times 3 \text{ cm}$ PMMA substrate (0.06 inch thick). In order to maintain consistency of experimental procedures, carbon paper was used as a cathode material for all tests. We fabricated $4 \text{ cm} \times 6.2 \text{ cm}$ PMMA supporting frame (0.5 inch thick) with the laser (Universal Laser System VLS 3.5) and drilled six holes for fluidic inlet/outlet and screws. Before we assembled the MFC, the anode/cathode chips were first sterilized with 70% ethanol and then blown dry with nitrogen. All layers were manually stacked in sequence while carefully aligning the tubing holes for the microfluidic channels. Four tubes (CODAN, 0.35 mL volume) were plugged into the holes to form two independent routes for anolyte/catholyte access.

PCL fibers were prepared by electrospinning, a versatile technique to produce nano/microfiber membrane because of its excellent dimensional controllability, highly macroporous non-woven structure, extremely high surface to volume ratio, wide variety of materials, one-step production of multi-coated nano/microfibers, etc. [19, 20]. In particular, the extremely high surface area and porous structure can lead to increased interaction with bacteria and, therefore, increased current density of MFCs. In this study, we have used poly(ϵ -caprolactone) (PCL) (Sigma-Aldrich, $\text{MW} = 90 \text{ kDa}$) as a fiber material, which has good biocompatibility and mechanical stability. The polymer solution dissolving 10 wt.% of PCL in 2,2,2-Trifluoroethanol (TFE) (Acros Organics, 99.8% purity) solvent was constantly fed at 1.2 mL h^{-1} by a syringe pump. High voltage $\sim 12 \text{ KV}$ was applied

across a gap of 20 cm between the needle and the collector. Because of very vigorous whipping and stretching actions of the ejected liquid jet, solidified fibers were attached to the collector.

2.4 Measurement Set-Up

We measured the potential between the anode and the cathode by a data acquisition system (National Instrument, USB-6212) and recorded the results every 1 min *via* a customized LabVIEW interface. An external resistor ($1 \text{ k}\Omega$), connected between the electrodes of the MFC, closed the circuit. We calculated current through the resistor *via* Ohm's law and the output power. Current and power density were normalized to the anode area (100 mm^2). We injected anolyte and catholyte to fill the $50 \mu\text{L}$ anode/cathode chambers by the syringe pump and we operated the MFC at the continuous mode.

3 Results and Discussion

3.1 Anode Materials for MEMS MFCs

The macroporous fiber anode was prepared on PMMA substrate. Resulting PCL fibers had a diameter of $\sim 1.1 \mu\text{m}$, with a standard deviation of $\sim 0.3 \mu\text{m}$ (Figure 2a). After electrospinning process, Denton mini-sputter system was utilized to sputter gold on electrospun fiber membranes for 10 min. No noticeable change in fiber diameter and membrane porosity was observed for the gold-coated PCL fibers. Interestingly, the gold coated PCL fiber membranes provide very low resistivity of $\sim 7 \times 10^{-3} \Omega \text{ cm}$, even though the sputtered gold does not fully cover the shadowed portion of the fibers. This electrical resistivity is comparable to that of carbon-based materials.

The current density of the fiber-based MFC was compared with gold and carbon paper anode MFCs (Figure 2b). Gold has been identified as a potential anode material for MEMS MFCs because it is highly conductive and is compatible with conventional microfabrication modalities. However, gold generated a very high anodic loss in MEMS MFCs increasing their internal resistance [9]. This indicated that the gold anode

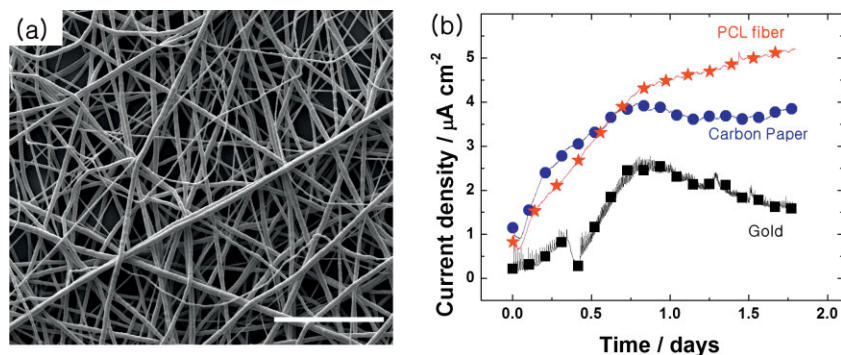


Fig. 2 (a) SEM images of the macroporous gold-coated PCL fiber (Scale bar is $30 \mu\text{m}$) and (b) currents produced from three MFCs, in which three anode materials are used (PCL fiber, carbon paper, and bare-gold).

was either toxic to the bacteria or otherwise poorly suited to interact with bacterial electron transfer [12]. On the other hand, carbon paper has typically been the material of choice for the construction of MFC anodes because it contains functional groups providing bacteria with more natural habitat. However, carbon paper is not suitable for MEMS MFCs because it is non-uniform and difficult to patterned in micro-scale devices. Therefore, it is worthwhile to compare our proposed anode to conventional representative two anode materials.

The same bacterial culture and potassium ferricyanide were continuously supplied to the anode and cathode chambers of three MFCs at the same time with flow driven by syringe pumps. Normally, the MFCs are operated under batch mode for the better accumulation and acclimation of bacteria on their anode surfaces [4, 9, 11]. Once current generation is observed after bacterial inoculation, media is supplied. However, as the size of the MFC is scaled towards the “micro” scale regimen, it is difficult to notice biofilm formation by monitoring its current generation because it becomes extremely sensitive to even minute O_2 levels interrupting bacteria from attaching to the surface for anodic growth and subsequent electron transfer, dramatically decreasing current generation [9]. That is why, we provided continuous and equal flow for all culture solutions for biofilm formation on the anode at a very low flow rate, $<1.0 \mu\text{L min}^{-1}$. This continuous operation helped keep a high flow by flushing out O_2 that had diffused into the anode, supporting better anode-respiration for the bacteria, ultimately decreasing start-up phase and increasing current density. Reducing oxygen diffusion is the key factor to increasing the performance of MEMS MFCs because O_2 diffusion into the anode chamber could compete with EET to the anode and, therefore, decrease coulombic efficiency and current generation [9].

The maximum current generated by the fiber anode was about $5.3 \mu\text{A cm}^{-2}$ while the carbon paper and gold produced smaller current densities, 3.8 and $2 \mu\text{A cm}^{-2}$, respectively. This is due to its ability to three-dimensionally interface with bacterial biofilm, promoting bacterial colonization and thereby facilitating electron transfer. The pore size of the PCL fiber is much larger than a bacterium (1–2 μm) and bacteria can easily diffuse in and colonize inside. Also, the macroporous structure of this fiber is expected to allow sufficient substrate exchange to support internal bacterial biofilm growth. The current from the gold anode gradually decreased once the current reached its maximum after 18 h. This result implies that gold material is not suitable for generating current from *Shewanella oneidensis* MR-1. The carbon paper-based anode produced much higher current than the gold anode but carbon-based materials are not suitable for MEMS MFCs because they are not compatible with necessary microfabrication processes and require manual assembly. In this sense, our fiber-based MEMS MFC will promote the realization of a microfabricated micro-sized MFC as a portable power source with a substantially upgraded power density. However, further study is necessary to determine whether the PCL fiber contains functional groups such as quinones.

3.2 Challenges in Scaling Down MFCs

The development of MEMS MFCs offers unique opportunities to reduce internal resistance and improve mass transport. However, miniaturization of the reaction chamber and channels also present challenges in developing and operating MEMS MFCs. The major challenges include unavoidable bubble invasion into the system and significantly sensitive effect of flow rate on performance, which have critical influence on EET process, mass transfer of anolyte catholyte, and biofilm formation. To date, these limitations have not yet been studied for high performance of MEMS MFCs. We prepared four PCL fiber anode based MFCs for these studies. Due to the difference of the initial number of bacteria from the one for the previous Section (3.1), the maximum current density of the four MFCs increased and reached a peak value of approximately $14 \mu\text{A cm}^{-2}$ with $<10\%$ variation (Data is not shown).

3.2.1 The “Bubble” Factor

While macro-sized MFCs are not vulnerable to invading bubbles, micro-sized MFCs become sensitive to even tiny air bubbles. This is because the size of the air bubble becomes comparable to that of chambers and the smaller number of bacteria in the anode are more susceptible to bubbles. Moreover, the trapped air bubbles are an enduring problem during the operation because they are difficult to be removed due to the slow flow rate of solutions. Therefore, the bubbles are expected to negatively affect the performance of MEMS MFCs. We investigated how bubble production could affect performance of the fiber-based MFC. As shown in Figure 3a, we intentionally introduced air bubbles into each chamber and maintained the system for 12 h with the bubble inside the chambers. In the anode microchamber, the current dropped by about 33% and it required 4 days to achieve maximum current density after a 12-h bubble interruption, while in the cathode recovery was almost immediate. This indicates that the EET and bacterial anode respiration might be seriously damaged or, some of bacteria might lose viability as the substrate was not fully supplied with the block of the trapped bubbles. Although this effect needs to be studied further to determine the cause, we can conclude that the air bubble invasion is one of the challenges that must be addressed in operating the MEMS MFCs.

3.2.2 Flow Rates

As the size of MFCs decreases down to micro-scale, the operating flow rates ($\mu\text{L h}^{-1} \sim \mu\text{L min}^{-1}$) are also significantly reduced from that in macro-scale MFCs ($\text{mL min}^{-1} \sim \text{L min}^{-1}$). Therefore, mass transfer flux and reaction kinetics on the electrode surface in MEMS MFCs can be actively altered by small changes in flow rates. Also, substrate and oxidant depletions are frequently observed under the slow flow rate because of the more efficient usage of substrates per unit volume with increased surface area for mass transport and reactions. We measured the current densities for the different flow rates of the anolyte and catholyte; 2, 5, 20, and

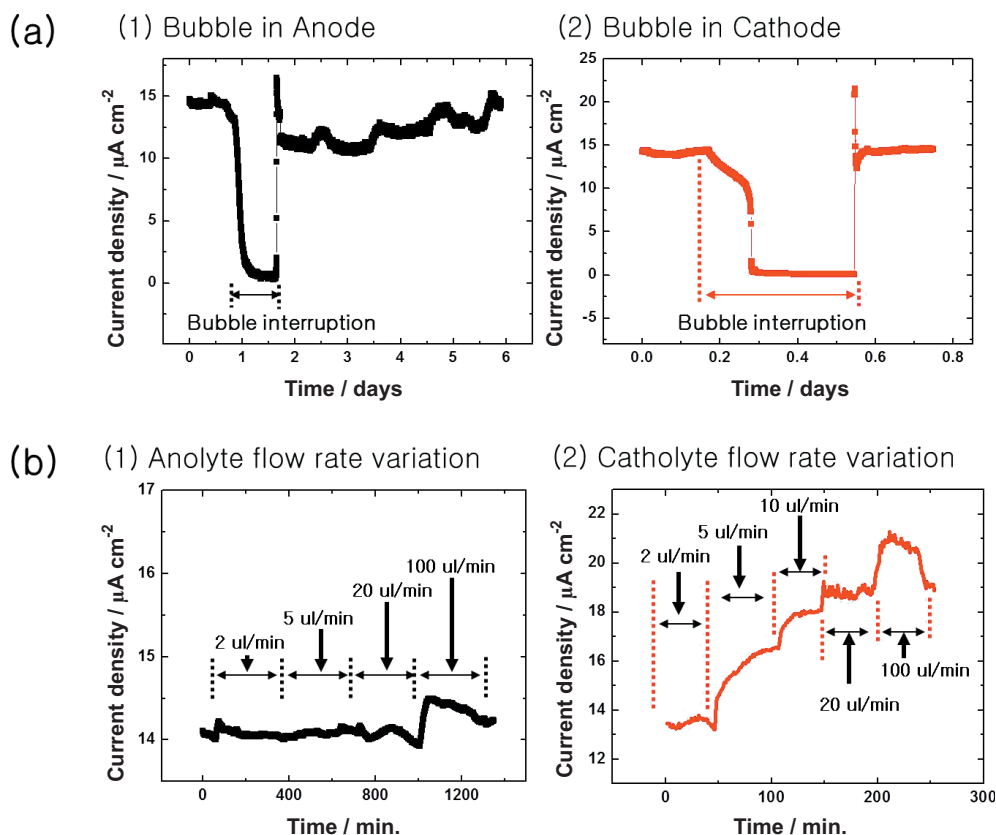


Fig. 3 (a) The role of potential bubbles in the (1) anode and (2) cathode micro-channels towards the current density of the PCL fiber-based MFC and (b) effects of the flow rates of (1) anolyte and (2) catholyte on the current density of the MFC.

100 $\mu\text{L min}^{-1}$. Although, the transient current generation was shown under 100 $\mu\text{L min}^{-1}$ because of sudden agitation, it dropped back to the base level. Generally, the current density was independent of flow rate in the anode chamber while the current densities increased with more rapid flow rate of cathode chamber. This result suggests that the MEMS MFCs do not suffer from the mass transfer loss of anolyte to provide more organic food to the bacteria. Rather, the concentration loss of catholyte and/or O_2 is a more dominant factor in the performance of MEMS MFCs. Although this experiment cannot provide the effect of flow rate on the biofilm formation because the biofilm was already fully formed, we can conclude that mass transfer of anolyte and metabolic bacterial behavior was not that affected by the microfluidic operation with different flow rates in MEMS MFCs. This is mainly due to the relatively slow rate of bacterial electron transfer process compared to that of cathodic reaction. Therefore, it is critical to address the cathodic limitation by increasing the catholyte concentration or the flow rate.

4 Conclusion

Here, we discussed the main limiting factors in developing and operating MEMS MFCs and provided suggestions to more effectively improve their performance. First, we proposed an alternative anode material for MEMS MFCs. The

gold-coated fiber based MFC produced higher current density than bare-gold and carbon paper based MFCs. This is because of the macroporous three dimensional structure which facilitates higher number of bacteria attachment. However, we expect that conformal coating of conducting material can be beneficial to obtain even higher conductivity of fiber membranes used for anodes in MEMS MFC devices, improving the performance. The proposed fiber anode will provide both compatibility to MEMS techniques and better surface characteristics for bacterial biofilm formation. Also, we studied two challenges in operating MEMS MFCs; bubble invasion, and high flow rate sensitivity. For high performance of MEMS MFCs, the concentration loss for catholyte and bubble interruption in the anode chamber must all be considered.

References

- [1] B. E. Logan, J. M. Regan, *Trends Microbiol.* **2006**, *14*, 512.
- [2] J. E. Mink, J. P. Rojas, B. E. Logan, M. M. Hussain, *Nano Lett.* **2012**, *12*, 791.
- [3] B. R. Ringeisen, E. Henderson, P. K. Wu, J. Pietron, R. Ray, B. Little, J. C. Biffinger, J. M. Jones-Meehan, *Environ. Sci. Technol.* **2006**, *40*, 2629.
- [4] F. Qian, M. Baum, Q. Gu, D. E. Morse, *Lab Chip* **2009**, *9*, 3076.
- [5] F. Qian, D. Morse, *Trends Biotechnol.* **2011**, *29*, 62.

- [6] C.-P.-B. Siu, M. Chiao, *J. Microelectromech. Syst.* **2008**, *17*, 1329.
- [7] H. Wang, A. Bernarda, C.-Y. Huang, D.-J. Lee, J.-S. Chang, *Bioresour. Technol.* **2011**, *102*, 235.
- [8] H. Ren, H.-S. Lee, J. Chae, *Microfluid. Nanofluid.* **2012**, *13*, 353.
- [9] S. Choi, H.-S. Lee, Y. Yang, P. Parameswaran, C. I. Torres, *Lab Chip* **2011**, *11*, 1110.
- [10] S. Choi, J. Chae, *Sens. Actuat. A* **2012**, DOI: 10.1016/j.sna.2012.07.015
- [11] S. Mukherjee, S. Su, W. Panmanee, R. I. Irvin, D. J. Hassett, S. Choi, *Sens. Actuat. A* **2013**, DOI: 10.1016/j.sna.2012.10.025
- [12] H. Richter, K. McCarthy, K. P. Nevin, J. P. Johnson, V. M. Rotello, D. R. Lovley, *Langmuir* **2008**, *24*, 4376.
- [13] F. Zhang, S. Cheng, D. Pant, G. Van Bogaert, B. E. Logan, *Electrochem. Commun.* **2009**, *11*, 2177.
- [14] G. Lepage, F. O. Albernaz, G. Perrier, G. Merlin, *Biore-sour. Technol.* **2012**, *124*, 199.
- [15] B. E. Logan, *Appl. Microbiol. Biotechnol.* **2010**, *85*, 1665.
- [16] S. Inoue, E. A. Parra, A. Higa, Y. Jiang, P. Wang, C. R. Buie, J. D. Coates, L. Lin, *Sens. Actuat. A* **2012**, *177*, 30.
- [17] L. Fitzgerald, E. Petersen, D. Leary, L. Nadeau, C. Soto, R. Roy, B. Little, B. Ringeisen, G. Johnson, G. Vora, J. Biffinger, *Biosens. Bioelectron.* **2012**, DOI: 10.1016/j.bios.2012.06.039
- [18] H. J. Kim, H. S. Park, M. S. Hyun, I. S. Chang, M. Kim, B. H. Kim, *Enzyme Microb. Technol.* **2002**, *30*, 145.
- [19] M. L. Alves da Silva, A. Martins, A. R. Costa-Pinto, P. Costa, S. Faria, M. Gomes, R. L. Reis, N. M. Neves, *Biomacromolecules* **2010**, *11*, 3228.
- [20] D. Han, A. J. Steckl, *Langmuir* **2008**, *25*, 9454.
-